EFDA–JET–CP(10)05/06

A.V. Chankin, W. Fundamenski, M. Groth, D. Moulton,
the ASDEX Upgrade Team, and JET EFDA contributors

Effect of Neutrals on the Power Decay Length at the Divertor Target

Effect of Neutrals on the Power Decay Length at the Divertor Target

A.V. Chankin[1], W. Fundamenski[2], M. Groth[3], D. Moulton[4],
the ASDEX Upgrade Team, and JET EFDA contributors*

JET-EFDA, Culham Science Centre, OX14 3DB, Abingdon, UK

[1]Max-Planck-Institut für Pasmaphysik, Boltzmannstraße 2, 85748 Garching bei München, Germany
[2]EURATOM/CCFE Fusion Association, Culham Science Centre, Abingdon, OX13 3DB, UK
[3]Helsinki University of Technology, Association EURATOM-Tekes, FIN-02015 HUT, Finland
[4]Imperial College London, Prince Consort Road, London, SW7 2AZ, UK
** See annex of F. Romanelli et al, "Overview of JET Results",*
(Proc. 22[nd] IAEA Fusion Energy Conference, Geneva, Switzerland (2008)).

Preprint of Paper to be submitted for publication in Proceedings of the
19th International Conference on Plasma Surface Interactions, San Diego, California, USA.
(24th May 2010 - 28th May 2010)

ABSTRACT.
EDGE2D modelling of JET divertor plasmas with wide variation of main plasma parameters was aimed at identification of operational domains of the applicability of the $2/7\times\lambda t_e$ scaling for predicting the power deposition profile width at the outer divertor target plate in high recycling conditions. Contrary to expectations, under no conditions, including lowest density plasmas just entering the conduction regime, was this scaling capable of correctly predicting the width and peak value of target power deposition profiles. Poorer ion parallel heat conduction, compared to the electron channel, in combination with reduced energy convection and volumetric power losses in divertor, of which charge exchange was found to play the dominant role, resulted in large deviations from the predictions of the $2/7\times\lambda t_e$ scaling.

1. INTRODUCTION

Narrowness of power deposition profiles at divertor target plates (q_t profiles) is a critical issue for ITER and future fusion facilities. Projections of today's experiments onto larger size, more powerful machines, together with fluid code simulations, show that the peak power load at the outer target is expected to be at the limit of present day technological capabilities for power exhaust [1].

The outer target receives most of the divertor heat load, with the smaller footprint compared to the inner target [1]. The scatter in the experimental dependences of the power width and the peak power density at the outer target however is large, even for different studies on the same machine [1]. This prompted theoretical studies for the ITER target power decay length scalings based on the so called "2-point model" [2]. According to this model, in the conduction regime expected in ITER, the decay length of the target power deposition profile λ_q,t is expected to scale with $2/7\times\lambda_{Te,u}$, where $\lambda_{Te,u}$ is the decay length of electron temperature upstream, reflecting the dominance of parallel electron heat conduction ($\propto T_{e,u}^{7/2}$) over that of the ions. Here $T_{eu,}$ is electron temperature upstream of the target, typically near the outer midplane, and large drop in T_e towards the target is assumed.

Multi-machine comparisons of H-mode upstream separatrix electron density (n_e) and temperature (T_e) profiles established a scaling law which, when projected onto the ITER size, predicts the T_e decay length at the outer midplane of about 2cm [3]. From here, the conduction power flow scale length, $\lambda_{q=}\ 2/7\times\lambda_{Te,u}$, for ITER is estimated to be of order 5-7mm [4].

Deviations from this scaling are expected in high density plasmas close to detachment due to recycling neutrals and impurity radiation in the divertor, with volumetric power losses spreading the target power over wider area [5]. Although, these effects were deemed to be relatively unimportant in low density well attached conduction regimes, where the $\lambda_{q=}\ 2/7\times\lambda_{Te,u}$ scaling was supposed to be upheld [1]. The present study demonstrates that direct target power deposition by volumetric power losses is not the only mechanism responsible for large deviation of the power deposition profile from that prescribed by the $\lambda_{q=}\ 2/7\times\lambda_{Te,u}$ scaling. Already at very low densities, when the plasma just enters high recycling conduction regime in the divertor, volumetric losses can influence plasma profiles (mainly of ions) in the divertor in a way that invalidates the predictions of the $\lambda_{q=}\ 2/7\times\lambda_{Te,u}$ scaling.

2. SETUP OF EDGE2D RUNS

The EDGE2D modelling described here is based on a well-diagnosed JET Ohmic discharge Pulse Number 56723 in MarkIISRP Gas Box divertor, with strike points on vertical targets. Original EDGE2D simulations of this discharge by Erents et al. [6] satisfactorily reproduced both upstream and downstream (at the outer target) experimental profiles. Further EDGE2D modeling in this JET equilibrium was made by Chankin et al. [7], after a significant refinement of the computational grid. The present results are based on the setup of [7]. Original transport coefficients of Ref. [6] were used: particle perpendicular diffusion coefficient $D_\alpha = 0.5 m^2 s^{-1}$, except for the region in the SOL between 1.6 and 2.8cm (mapped to the outer midplane position) where D_α is raised up to $1.5 m^2 s^{-1}$, and ion and electron perpendicular heat conductivities $\chi_i = \chi_e = 3D_\alpha$. For further details such as fuelling and exhaust options the reader is addressed to Ref. [7]. The density and input power in the present study were varied to cover wide range of divertor conditions: separatrix electron density was varied from 0.27 to $1.3\times10^{19} m^{-3}$ in Ohmic plasma conditions with P_{input}= 1.6MW, and from 1.1 to $3.6\times10^{19} m^{-3}$ – in H-mode conditions with P_{input} = 12MW. Input power was equally shared between ion and electron channels. All cases were run without drifts. Eirene 96 neutral Monte-Carlo package was used. Gas puffing from outside was used to control density. Realistic chemical sputtering coefficients were used for carbon radiation. Heat flux limiters were not set.

3. MODELLING RESULTS

Figure 1 shows power density profiles at the Outer Target (OT), split into contributions from separate ion and electron channels and radiation (including charge-exchange neutrals), Outer MidPlane (OMP) and OT profiles of T_e and T_i, in a series of EDGE2D runs with low (Ohmic) input power and rising separatrix density (n_s). The lowest density case (top diagrams) can be qualified as corresponding to low density high recycling regime, with a 60% T_e drop from OMP to OT. For even lower n_s, the plasma is in the sheath-limiting regime. Despite $T_i >> T_e$ at OMP, target T_i drops to levels substantially below T_e near the strike point. Correspondingly, power deposition flux density due to ions also drops towards the strike point, resulting in the total deposition profile (carried mostly by ions and electrons, with negligible contribution from radiation) being almost flat across the region that covers > 50% of the total power deposition onto the target. Also shown is the profile of the target power following from the $q_t \propto T_{e,u}^{7/2}$ dependence and normalized so as to give the same total power as the EDGE2D-extracted "total power" shown in the figure. Instead of just taking the T_e at OMP, the difference $(T_{e,OMP}^{7/2} - T_{e,OT}^{7/2})/L_\parallel/Z_{eff}$, with $L_\parallel$ being the connection length from the OMP to the target, and Z_{eff} – actual code value for the OMP, was used. In addition, the target profile was corrected for the variation (albeit, rather small) in the flux expansion factor between OT and OMP positions along the field lines.

There are a number of reasons for large drops in T_i and ion target power towards the strike point at the outer target. First, the conductive ion power flux to the outer divertor is much less than the electron power flux owing to much lower ion parallel heat conduction: $\chi_{i,\parallel} << \chi_{e,\parallel}$. At the same

time, the convective ion power flux is reduced owing to high recycling conditions in the divertor. High recycling leads to a significant drop in the Mach number of the parallel ion flow. As shown in Figure 2, this drop is particularly large for low and medium density cases in the vicinity of the strike point, where most of the power on the target is found. Some increase in the Mach number is seen in the high density case, which is probably related to detachment at the target.

Figure 3 shows poloidal energy flux by ions and electrons at the entrance to the outer divertor, together with the poloidal electron power flow, directly calculated according to the $q_t \propto T_{e,u}^{7/2}$ law, using local T_e values at OMP and at the entrance to the outer divertor. While electron power flux into the divertor approximately follows the $q_t \propto T_{e,u}^{7/2}$ law, the ion flux profile differs substantially from it, being also numerically much smaller.

Power loss mechanisms for the lowest density Ohmic case are listed in Table 1. Powers are summed up over grid cells belonging to the outer divertor region ("outer divertor SOL" region, according to nomenclature adopted in EDGE2D). The largest power loss mechanism for ions is Charge Exchange (CX). Owing to its localization around the strike point position, it is very effective in reducing T_i over the region where most of the power flux on the target is found. Each ion-neutral (atom) collision reduces ion energy to a very low level, which is impossible to compensate by ion heat conduction. The result is a large drop in T_i and an increase in plasma density (in order to sustain plasma pressure balance along field lines), leading to an amplification of the target particle flux (high recycling of neutrals). High recycling in the divertor slows down plasma flow to the divertor thereby reducing convective ion energy flux. In addition to this, CX serves as an important direct power loss mechanism, reducing ion power flux to the target.

As the separatrix density is raised, producing first medium density partially detached (middle diagrams in Fig. 1) and then high density strongly detached (bottom diagrams in Fig. 1) plasmas in the divertor, the role of radiative power deposition onto the target is also increased. However, until high density strongly detached conditions in the divertor are reached, most of the power deposition onto the target is still due to charged particles (ions plus electrons). Only at high densities the direct power deposition by volumetric power losses becomes dominant (see bottom left diagram in Fig. 1). In all cases, except for lowest density ones, ion and electron target power profiles remain "inverted" (with the power density rising away from the strike point) over the region where > 50% of the total target power is deposited, and shapes of power deposition profiles have little resemblance to those predicted by the $q_t \propto T_{e,u}^{7/2}$ law.

A similar situation regarding target profiles is seen in the low density high power case shown in Figure 4. CX losses (-4.15E-01MW) are even more dominant than in low power cases, significantly exceeding the combined electron losses on impurity and hydrogen radiation (-1.61E-01MW), and representing 8% of the total power flow to the outer divertor (5.2MW). CX losses, as mentioned above, are strongly localized in the vicinity of the strike point, providing strong local energy sinks.

For the high power, high density case with strong detachment, shown in Fig. 5 (similar to the situation in high density low power case), CX losses are not dominant (-7.26E-01MW), being

smaller than electron radiative losses (-1.09MW). Radiative target power load accounts for about a half of the total power load; T_e and T_i are strongly linked to each other by equipartition.

It is worth noting that the ratio of the peak power densities: predicted according to the $q_t \propto T_{e,u}^{7/2}$ law, and modelled with EDGE2D, is even higher for low density cases (2.69 and 2.60, for high and low input powers, respectively), than for high power density cases (1.96 and 2.35, for high and low input powers, respectively), emphasising the fact that low density cases are not anywhere nearer in terms of matching the $q_t \propto T_{e,u}^{7/2}$ profiles than high density cases.

Ratios of outer target power widths modeled with EDGE2D and predicted according to the $q_t \propto T_{e,u}^{7/2}$ law, as a function of the latter, are plotted in Fig. 6. Power widths are calculated as integrals of the power to the target divided by the maximum power density. The ratios are of order 2 – 2.5, on average, indicating the degree of actual power spread over the target compared to predictions of the $q_t \propto T_{e,u}$ law.

4. SUMMARY

There seems to be no window in divertor operating conditions where the $q_t \propto T_{e,u}^{7/2}$ law for divertor target power deposition profiles can be applied. In high density detached conditions, where divertor power load is dominated by radiative losses, a much wider power spread over the target is seen in the present EDGE2D modelling, with the peak power reduced by factor ~ 2, as expected. Contrary to the expectations, however, even in lowest density cases (but in high recycling regime, ensuring conductive electron power losses), modelled target power profiles have little resemblence to predictions of the $q_t \propto T_{e,u}^{7/2}$ law. In the EDGE2D low density cases, ratio of the peak power densities: predicted according to the $q_t \propto T_{e,u}^{7/2}$ law, and modelled, is even higher for low density cases than for high density ones. One reason for the disagreement with this law is a much lower parallel ion heat conduction than that of electrons, with the ion power deposition profile influenced by local (at each flux surface) convective power flux which in turn is strongly influenced by recycling in the divertor.

As soon as high recycling conditions in the divertor are set in, power losses associated with plasma-neutral interactions start strongly influence target power profiles. CX power loss, which is the dominant loss mechanism for ions, causes dramatic reduction of target T_i near the strike point. This increases local plasma density (due to the tendency of the total pressure to reach equilibrium along field lines) and the level of recycling, reducing convective power flows to the divertor. At low to medium densities, most of the target power deposition is via ion and electron channels (role of volumetric losses' power load is small), and the influence on the target power profiles is via an "inversion" of $T_{e,i}$ profiles (drop towards the strike point, along the target).

Based on the limited set of simulations, it appears that the $q_t \propto T_{e,u}^{7/2}$ law underestimated the integral power width on the target by a factor 2 to 2.5.

ACKNOWLEDGEMENT

This work, supported by the European Communities under the contract of Association between

EURATOM and Max-Planck-Institut für Pasmaphysik, was carried out within the framework of the European Fusion Development Agreement. The views and opinions expressed herein do not necessarily reflect those of the European Commission. We would also like to acknowledge Profs. R.J. Goldston and P.C. Stangeby for motivating this study and for interesting duscussions.

REFERENCES

[1]. Loarte A et al., "Progress in ITER Physics Basis", Chapter 4: "Power and Particle Control", Nuclear Fusion **47** (2007) S203-S263.

[2]. Borrass K, Nuclear Fusion **31** (1991) 1035.

[3]. Kallenbach A, et al., J. Nuclear Materials **337-339** (2005) 381.

[4]. Lipschultz B, et al., "Plasma-Surface Interactions, Scrape-Off Layer and Divertor Physics: Implications for ITER", Proc. 21st Fusion Energy Conference, IAEA, Nuclear Fusion **47** (2007), IT/1-4, special issue, http://www-naweb.iaea.org/napc/physics/FEC/FEC2006/html/index.htm.

[5]. Borrass K, J. Nuclear Materials **290-293** (2001) 551.

[6]. Erents S K, et al., Plasma Physics and Controlled Fusion **46** (2004) 1757.

[7]. Chankin A V, Coster D P, Corrigan G, et al., Plasma Physics and Controlled Fusion **51** (2009) 065022.

species	Impurity radiation	Hydrogen radiation	CX	equipart.	atom. ioniz.	molecular ioniz./diss.
electr.	-6.76E-02	-1.30E-02	-	+1.66E-02	-1.57E-02	-2.52E-02
ions	-	-	-5.89E-02	-1.66E-02	+2.00E-02	+3.24E-03

Table 1. Break-up of ion and electron power loss channels (in MW), integrated over the outer divertor SOL region, for the Ohmic case with $n_s=0.4\times10^{19}m^{-3}$.

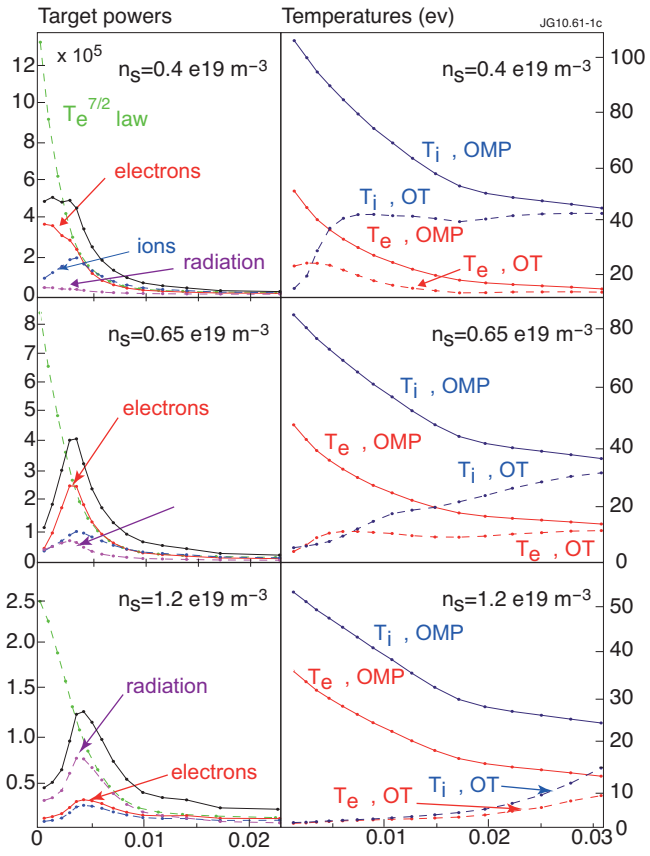

Figure. 1. Target power, upstream and target T_e and T_i profiles for a series of EDGE2D runs with different separatrix densities (n_s) at Ohmic input power.

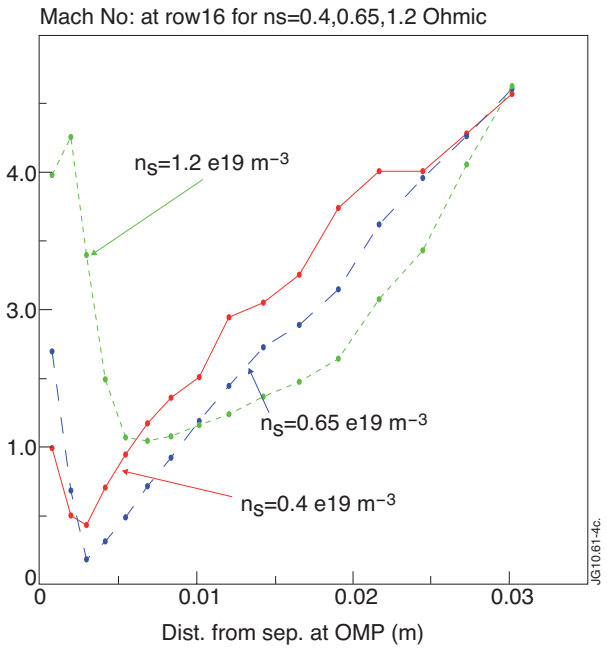

Figure. 2. Mach numbers of the parallel ion flux at the entrance to outer divertor for three levels of separatrix density at low (Ohmic) input power.

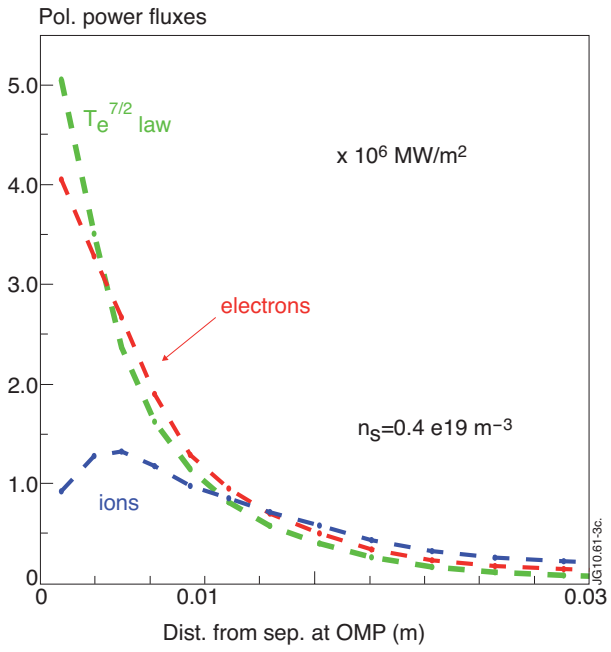

Figure. 3. Poloidal power flux profiles at the entrance to outer divertor, for the low density Ohmic case.

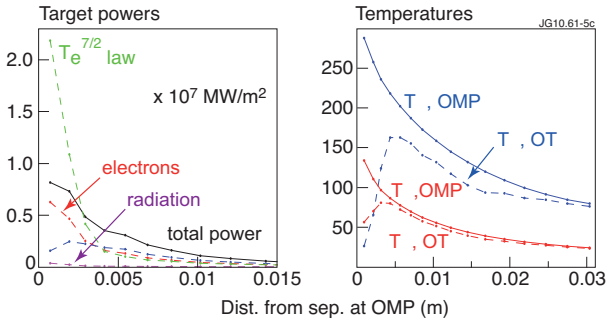

Figure. 4. Same quantities as shown in Figure. 1, but for low density (n_s=1.1×10^{19}m^{-3}) case with high (12MW) input power. Note different horizontal axes on the diagrams.

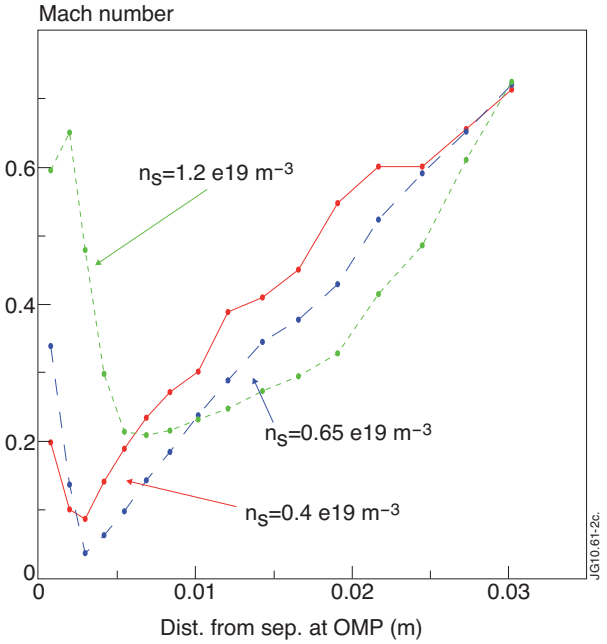

Figure. 5. Same quantities as shown in Fig. 1, but for high density (n_s=3.6×10^{19}m^{-3}) case with high (12MW) input power.

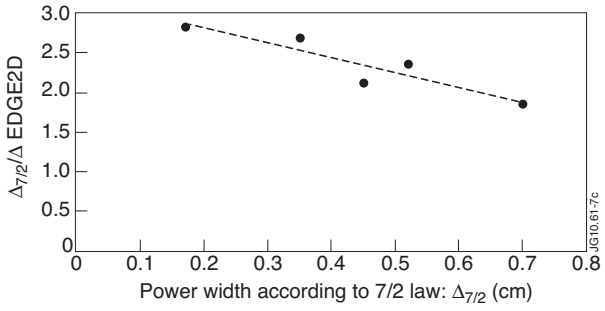

Figure. 6. Ratio of outer target power widths modeled with EDGE2D and predicted according to the $q_t \propto T_{e,u}$ law, as a function of the latter. Distances are projected onto OMP position. Cases plotted are (in ascending order, along X-axis): low density high power; low, medium and high density Ohmic, high density high power.